SILICONE OPTICALLY CLEAR ADHESIVE FOR ELECTRONIC APPLICATIONS

Kwanho Chang, Staff Scientist, Momentive Performance Materials, Waterford NY
David Newsham, Staff Scientist, Momentive Performance Materials, Waterford NY

Abstract

Bonding optical components is vital to the consumer electronics, automotive, and photovoltaic industries. Bonding is especially critical in touch-screen devices. Screen durability and viewability can be significantly affected by how the layers that make up a typical screen such as the cover window, touch sensor and display module are bonded together.

Bonding can be achieved through several different processes. One of the most effective methods of optical bonding is laminating the functional layers with a cured, optically clear adhesive (OCA) film. OCAs are pressure sensitive adhesives formulated into a transferrable film sandwiched between release liners. The use of a transfer adhesive film allows for good control of film thickness and more rapid assembly than is generally possible with conventional optically clear resins (OCR), which are typically applied as a liquid and require custom processes and potentially longer post cure periods.

Silicone OCAs offer the advantages of silicone adhesives. Silicone's exceptional UV resistance and chemical/mechanical stability over a broad temperature range enable silicone OCAs to perform in many environments, including the harsh conditions that are often associated with aerospace and automotive applications. In addition, the tunable modulus and T_g allow silicone OCAs to be optimized for performance in a wide variety of applications.

This paper will discuss the development of silicone OCAs for use in electronics applications.

Introduction

Bonding optical components is of importance in the consumer electronics, automotive, and photovoltaic industries.[1] Bonding is especially critical in touch-screen devices, which have shown substantial growth during the past decade. The durability and performance of a screen can be significantly affected by how the internal layers, such as the cover window, touch sensor and display module, bond together within the device.

Bonding can be achieved by laminating the functional layers with a pre-cured, optically clear adhesive (OCA) film. OCAs are optically transparent, pressure sensitive adhesives (PSA) that are typically made of either acrylic or silicone materials and formulated into a transferrable adhesive film sandwiched between release liners. The use of a transfer adhesive film allows for good control of film thickness even in the case of curved-to-curved surface bonding and enables more rapid assembly than is generally possible with conventional optically clear resins (OCR), which are typically applied as a liquid and require a longer post cure period. In addition to bonding the display layers, the use of OCA offers the major benefit of enhancing viewability of the displays by filling air gaps present under the cover window. The OCA minimizes light reflection/ refraction caused by the refractive index mismatch between adjacent layers, which leads to extension of a battery life.

Although commercially available OCA tapes are primarily based on acrylic materials, silicone OCA has drawn growing attention for emerging applications due to its distinct properties over acrylic OCA.[2] Silicone OCAs present not only the advantages typical of silicone adhesives, but also advanced features relevant to electronic applications. Silicone's exceptional UV resistance and chemical/mechanical stability over a broad range of temperature as well as low modulus and exceptional elasticity at subzero temperature make it a versatile solution that can meet the challenging requests presented by a variety of applications, including those of extremely demanding aerospace and automotive applications.

The physical properties of silicone OCA are readily tunable to fit the application requirements by blending varying amounts of two major components: high molecular weight silicone gum and highly branched silicone resin.[3] Silicone gum takes the form of a linear polymer composed of divalent D units [$R_2SiO_{2/2}$] and is represented as *soft* segments to ensure consistent operation at extremely low temperature due to the glass transition temperature (T_g) of *ca.* -120 °C. Silicone resins are condensed silicates with relatively low molecular weight and normally referred to as MQ resins, as they consist of monovalent M units [$R_3SiO_{1/2}$] and tetravalent Q units [$SiO_{4/2}$]. They are represented as *hard* segments with very high T_g, over 300 °C, and responsible for peel strength and shear adhesion at high temperatures. When silicone resins are dissolved with silicone gum in solvent, dried, and cured into an adhesive film, the resulting article will exhibit two separate glass transition temperatures as it forms a partially miscible or micro-phase separated mixture caused by dissimilarity in molecular structure. The T_g of the silicone gum remains at -120 °C while the T_g of the MQ resin drops substantially according to the resin-to-gum (R/G) ratio. In comparison, acrylic OCA shows only a single T_g although it is constructed with a similar concept of hard and soft segments.[3] Therefore, silicone OCA can be formulated to exhibit the elastic modulus orders of magnitude lower than acrylic OCA as shown in Figure 1.

Unlike traditional silicone PSA cured with benzoyl peroxide, silicone OCA is generally addition-cured: platinum catalyzed hydrosilylation of vinyl silicone with hydride crosslinker.

Silicone gums can be vinyl end-stopped or mid-functional. MQ resins can also be functionalized to react with hydride cross-linker. Accordingly, addition cure OCA can allow for more precise control of the polymer network structure and lower cure temperature than peroxide-cure.

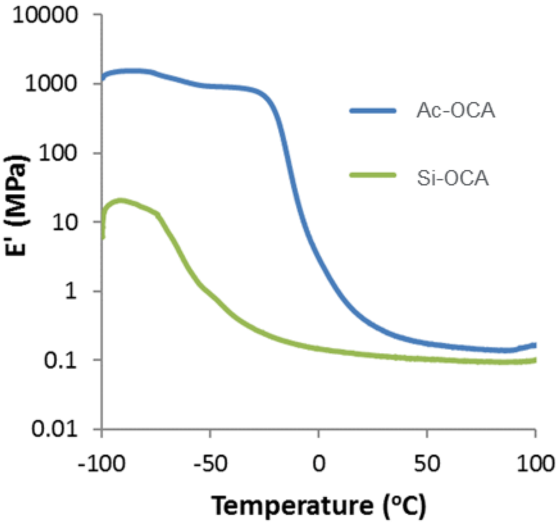

Figure 1. Elastic modulus of acrylic OCA (Ac-OCA) and silicone OCA (Si-OCA)

When it comes to the electronic applications that require dynamic performance, such as flexible displays and touch sensors,[4] peel adhesion strength of silicone PSA can be balanced with adhesive elasticity by optimizing the amount of MQ resin in the formulation. The parameters of rheological properties, e.g., elastic modulus (G′), loss modulus (G″), and tan δ (= G″/G′), become keys to altering dynamic performance of silicone OCA within an operating temperature window. This paper will discuss the developmental efforts to place silicone OCA in various consumer electronics, in particular, those that emphasize the need for specific dynamic features.

Experimental

Preparation of Silicone OCA Coatings

All compositions were dissolved in toluene and coated onto a 2-mil fluorosilicone release liner using a Gardner applicator in a motorized coating station. The coated samples were dried at ambient temperature for 20 min, cured in oven at 135 °C for 5 min, and covered with the fluorosilicone liner. The thickness of the cured films was targeted to either 25 μm or 100 μm, depending upon the test conditions.

Dynamic Mechanical Analysis (DMA)

The rheological properties of the adhesives were measured using either DMA-Q800 (TA Instruments) in an extensional mode or ARES-G2 (TA Instruments) in a shear mode. The specimens were prepared by stacking multiple OCA films using a rubber roller and cutting them into a 5.3 mm × 30 mm rectangular strip using a hand-cutter supplied by the original manufacturer. The trimmed samples were annealed for at least 24 hours before DMA testing. Dynamic strain sweep was performed to determine a critical strain in a linear viscoelastic (LVE) regime. The temperature ramp experiments were carried out from -100 °C to 150 °C at a rate of 3 °C/min under an oscillatory deformation with a strain of 0.1 % and a frequency of 1 Hz. As a result, loss modulus (E″ or G″), storage modulus (E′ or G′), and tan δ, which is defined as the ratio of loss to storage modulus, are reported.

Cyclic Deformation Test

The OCA tapes were stacked to a 1mm thick film using a rubber roller as described previously and punched into dog bones using a dumbbell cutter in accordance with JIS K6251-2. After the specimen was installed in Instron tension meter (model 3366), an upper clamp pulled the specimen to a pre-determined strain (%) at a crosshead speed of 500 mm/min and returned to the original position. After 10 cyclic deformations, the strain was step-increased to a higher strain up to 400%. Tensile strength and energy under the stress-strain curve were calculated from the measurements.

180° Peel Adhesion and Release Force

Peel tests were performed using TA.XT Plus texture analyzer (Stable Micro Systems™). To measure peel strength, 25mm wide strips of OCA tape were transferred to PET films and applied on stainless steel panels under a standard 2 kg loading. After 30 minute dwelling, the OCA tape was clamped and pulled vertically from the panel at 180° angle at a rate of 300 mm/min until the tape was delaminated from the panel by 60 mm. The force recorded at a steady state was time-averaged. All reported data are the average of three replicas. For release force test, a tight liner was directly peeled from the adhesive attached to the stainless steel panel.

Static Bending Test

25 µm polyimide (PI) films and 100 µm OCA tapes were cut into 104 mm × 76 mm rectangles, assembled together into a PI/OCA/PI tri-layer and mounted on two adjacent 76mm × 52mm slide glasses as shown in Figure 2. Then one side of the sample was folded inward and clamped over a 5mm thick spacer to hold the curvature. The completed assembly was aged at 60°C /90%RH in a humidity chamber and visually inspected after 24 hours.

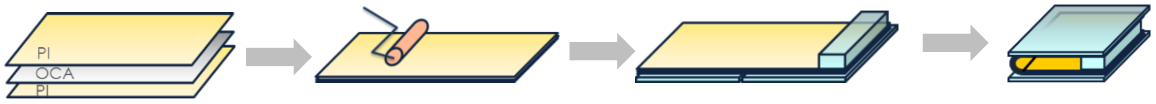

Figure 2. Schematics of sample preparation for static bending test.

Outgas test

The tri-layer samples for the outgas test were prepared by laminating the OCA tape between plastic films. Initial defects or voids present on the laminated samples were marked in black. The samples were placed at 85°C /85%RH in a humidity chamber for 1 hour and photographed to count the number of blisters that appeared on the surface.

Results and Discussion

In order to assure the low temperature flexibility, the glass transition temperature of the OCA needs to locate below the operating temperature window. Figure 3(a) plots tan δ curves of silicone OCA comprised of silicone gum and MQ resin at various R/G ratios. As the amount of MQ resin was reduced in the composition, not only did T_g drop in proportion to the R/G ratio, but also both the peak and plateau values of the tan δ curve decreased accordingly in magnitude, implying that the OCA becomes more rubbery and elastic. Also, Figure 3(b) shows that the plateau values of tan δ can be easily shifted while fixing the location of peak tan δ, or T_g, by using a different type of silicone gum.

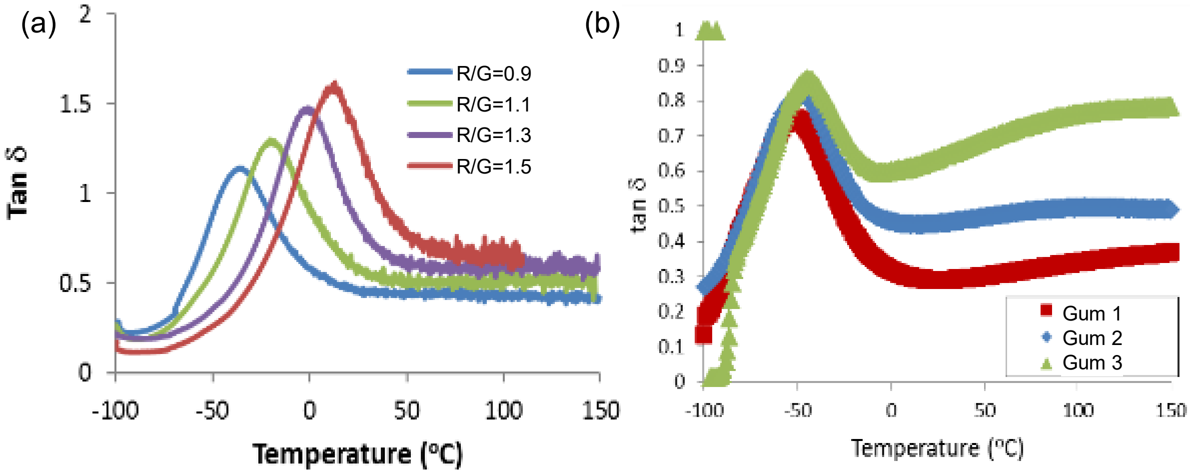

Figure 3. tan δ curve of silicone OCA prepared with (a) a varying R/G ratio and (b) different silicone gums.

For a given thickness of the OCA, Figure 4 shows that peel strength of silicone OCA and release force of the tight liner linearly decrease with a decreasing R/G ratio. The change was more pronounced with thicker OCA samples. The force difference between 1 mil (25 µm) and 3 mil (75 µm) OCAs was least at the lowest R/G ratio and greatest at the highest R/G ratio. It is noteworthy, however, that further decrease in the R/G ratio did not cause a crossover but a leveling off of both peel strength and release force. As the influence of MQ resin becomes marginal in the OCA film, the overall properties will be primarily determined by the silicone gum phase via crosslink density or plateau moduli.

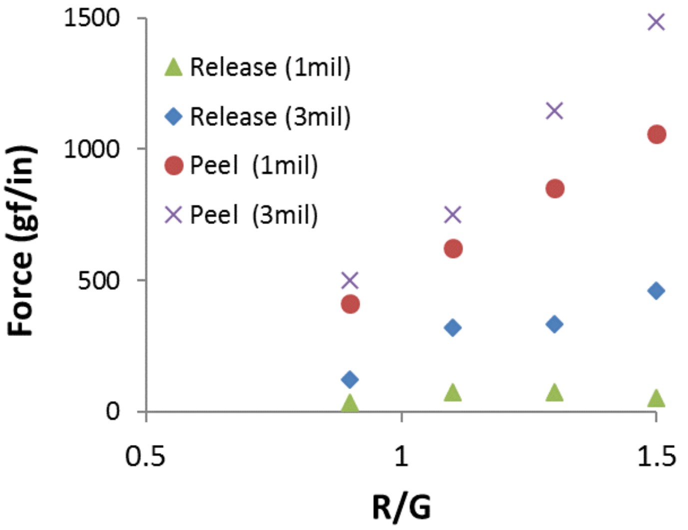

Figure 4. Peel adhesion strength of silicone OCA and release force of a tight liner as a function of the R/G ratio.

Hysteresis analysis was conducted on both acrylic and silicone OCA films by applying the cyclic extensional deformation. The area of the hysteresis loop is associated with the amount of energy dissipated upon reversal of the force, which in turn involves an adiabatic exotherm. As shown in Figure 5, the largest permanent set, or *stress softening*, occurred during the first load/unload process showing the widest hysteresis loop. From the subsequent load/unload cycle the hysteresis loop decreased in size but remained identical during the remaining cycles, indicating that pure elastic behavior prevailed the following deformation. Such irreversible stress softening is referred to as “Mullins effect” and often reported in filled rubber systems.[5] When the sample was extended to a new strain beyond the maximum stretch previously applied, the stress softening process started over again.

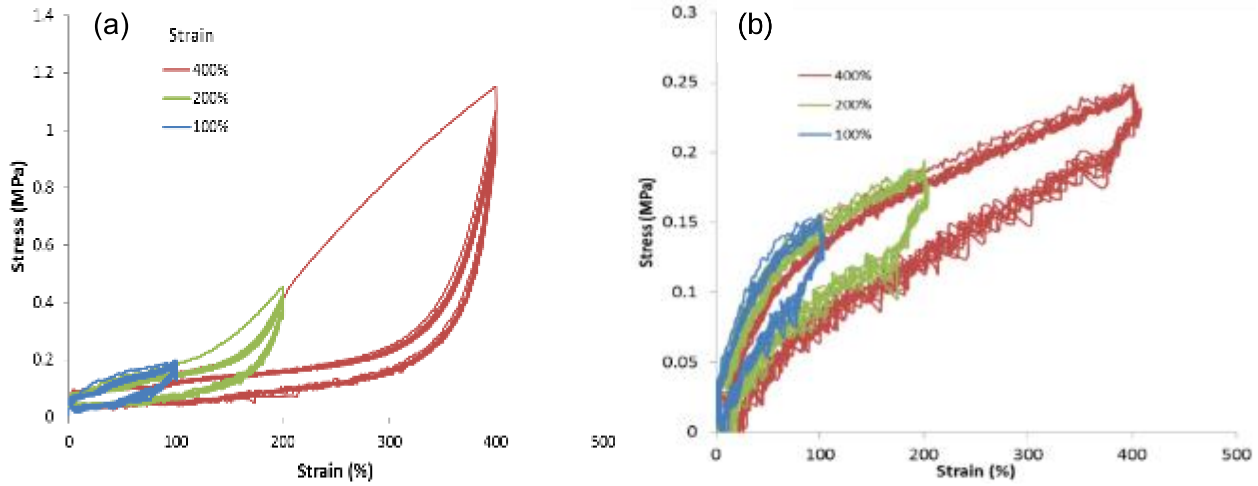

Figure 5. Stress-strain curve from cyclic deformation: (a) acrylic OCA and (b) silicone OCA

Figure 6 compares stress softening of the OCAs, which is defined as a ratio of the area difference in the hysteresis loop between the first and last cycle to the area of the first hysteresis loop. It accounts for permanent energy loss during cyclic deformation. Stress softening appeared even more significant in acrylic OCA compared to silicone OCA with the similar T_g. Stress softening progressively increased with increasing strain for acrylic OCA while it remained nearly unchanged for silicone OCA.

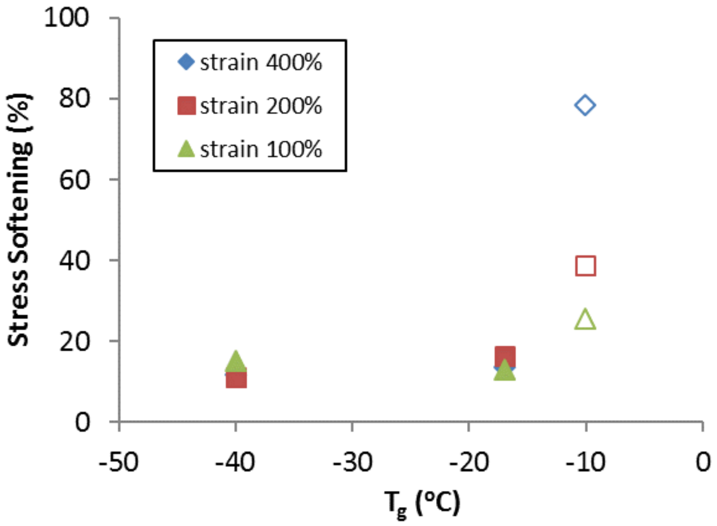

Figure 6. Stress softening of acrylic OCA and silicone OCA at various extensional strains. Filled symbols: silicone OCA, hollow symbols: acrylic OCA

Also, nano-indentation testing was utilized to evaluate the elasticity of acrylic and silicone OCA tapes. A 0.4 mm ball indenter was used to compress the OCA film combined with plastic substrates under variable loads, which was ramped at a rate of 1mN/3sec, held at the maximum for 5 sec, and released. The OCA films experienced variable extents of creep at the maximum load as presented in Figure 7(a). Silicone OCA showed the similar load-to-depth profile to silicone OCR, but outperformed all acrylic OCAs showing higher displacement depth, less creep, and higher percentage recovery. Further investigation elucidated that creep distance is inversely proportional to the elastic modulus in Figure 7(b). Therefore, careful control of the elastic modulus OCA is necessary to meet the needs in electronic devices.

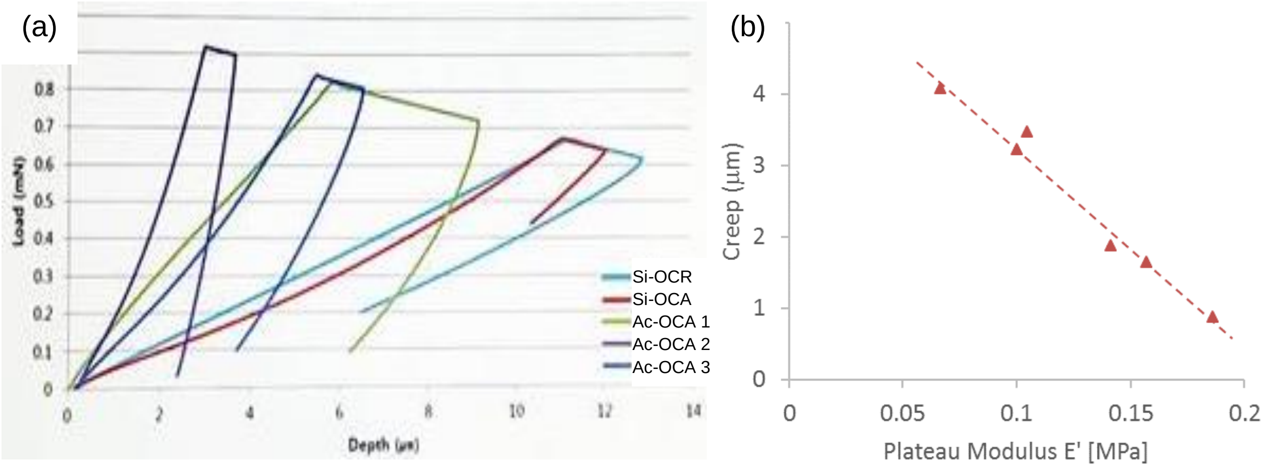

Figure 7. (a) Nano-indentation results of silicone OCA (red) in comparison with silicone OCR (blue) and acrylic OCAs (condition: 0.4mm ball indenter, 1 mN/3 s, creep 5 s) (b) creep distance as a function of plateau modulus.

In addition to the aforementioned extension and compression behaviors, we also attempted to probe bendability of silicone OCA using an in-house experimental setup as a substitute dynamic bending test. The experiments were performed by folding the PI/OCA/PI tri-layer assembly in a static condition under a fixed curvature at 60 °C/90%RH for 24 hours. Table 1 summarizes the static bending test results of two representative silicone OCA samples. After 24 hour aging, Sample 1 came out free of surface defects, whereas Sample 2 suffered from delamination on the central zone where the most stress was concentrated. It was obvious that the failure of Sample 2 was not caused by low peel strength. Instead, it turned out that the rheological properties, in particular a plateau tan δ value, at high temperature had a great influence on bending resistance. Figure 8 plots plateau tan δ values of silicone OCA samples with 100 μm thickness as a function of the R/G ratio. Test results are highly segregated into two regions over a wide range of the R/G ratio. All OCA samples with plateau tan δ values greater than 0.5 passed the static bending test. On the other hand, those with plateau values less than 0.4 failed the test yielding delamination (adhesive failure) at the center. No cohesive failure of the film was observed. Accordingly, one can explain the previous result given in Table 1 emphasizing the effect of the viscous component of the OCA tape on dissipating bending energy in the region under stress so as to present adhesive failure.

Table 1. Static bending results of silicone OCA sandwiched between PI films

	Sample 1	Sample 2
t = 0 h		
t = 24 h 60°C/90%RH		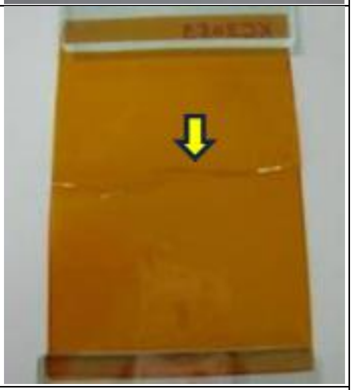
Bending test	Pass	Adhesive failure
Peel adhesion	590 gf/in	740 gf/in
Plateau tan δ	0.53	0.32

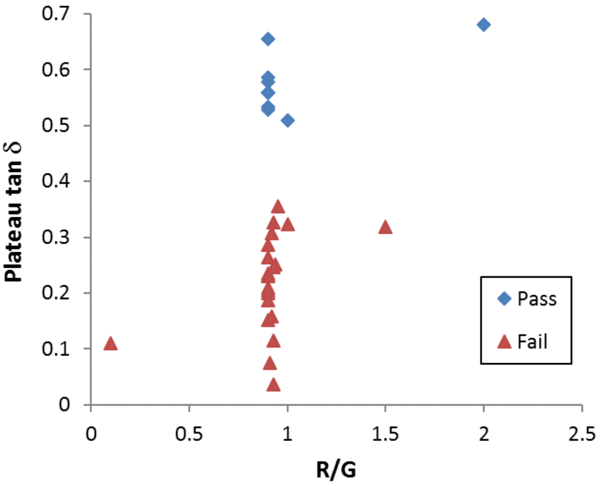

Figure 8. Static bending test results of silicone OCA (100 μm) as a function of plateau tan δ

Apart from adhesive properties, another important aspect to be taken into account for silicone transfer adhesive is release force from a fluorosilicone liner. Release force is largely determined by surface energy difference between materials used in coating on the liner and adhesive film[6], but also closely related to wettability of the adhesive on the liner surface. Therefore, release force tends to increase with loss modulus or tan δ values.[7] Too great a release force may cause transfer failure of the OCA film on the adherend surface, especially in the automated process. Figure 9 shows the effect of plateau tan δ values on release force of a tight liner measured with silicone OCA. As expected, release force decreases rapidly with decreasing plateau tan δ values and then becomes saturated if the OCA becomes sufficiently elastic with low tan δ. In order for silicone OCA to be used in applications requiring extreme bending performance, it is essential to balance release force with bending resistance by careful control of the rheological properties of the adhesive.

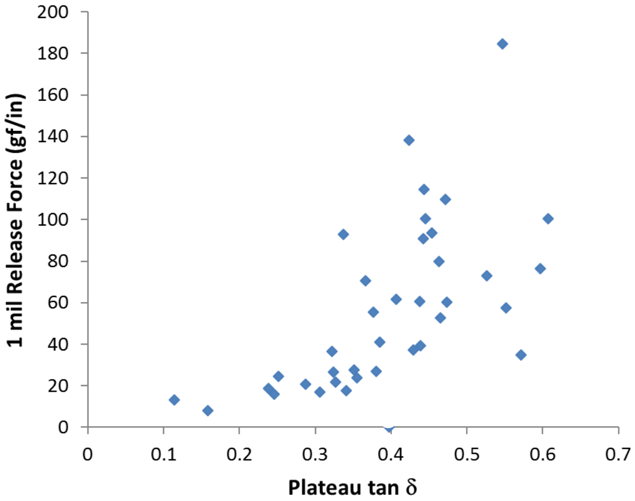

Figure 9. Release force of a tight liner of silicone OCA as a function of plateau tan δ

Outgassing or blistering of OCA films laminated with plastic substrates has been reported in literature[8,9] when it was exposed to high temperature and high humidity conditions. In cases with acrylic OCA, such defects are primarily caused by moisture present in the adhesive and substrates, and the proposed solution is addition of an acrylic tackifier to increase peel strength. Outgassing of silicone OCA is a more complex problem because addition-cured silicone OCA contains residual hydride that can react with moisture to generate hydrogen gas as described below.[10]

$$2 \equiv\mathrm{SiH} + \mathrm{H_2O} \longrightarrow \equiv\mathrm{Si{-}O{-}Si}\equiv + 2\,\mathrm{H_2}\uparrow$$

Therefore, it is vital to remove residual hydride in the cured silicone OCA. In addition, silicone is more hydrophobic in nature than acrylic material due to non-polar composition of the polymer back bone so that the solubility of water in the silicone OCA is considerably lower than that in acrylic OCA. It was observed that addition of hydrophilic additives in silicon OCA could mitigate the outgas issue to a certain degree depending upon molecular structure of additives (0.8 wt %) as illustrated in Figure 10. Also, it was confirmed that outgas resistance of silicone OCA was dramatically amplified by optimizing the lamination process conditions, which will require the close collaboration with the end user to develop a tailored process to apply silicone OCA in the electronics applications.

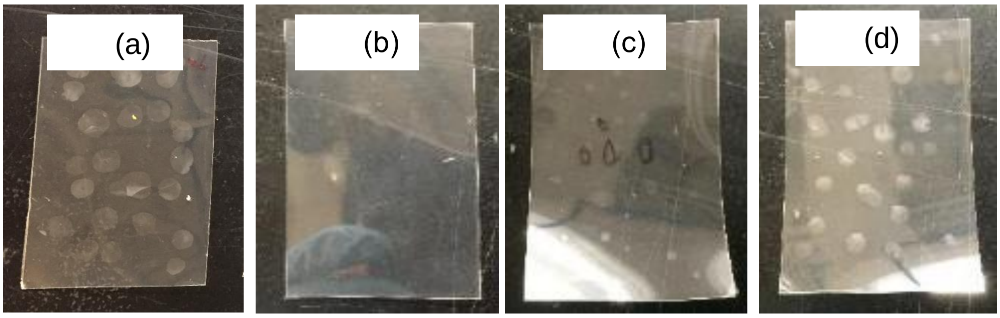

Figure 10. Outgas test results of silicone OCA laminated with PET films in the presence of (a) no additive (b) additive 1 (c) additive 2 (d) additive 3

Conclusion

Silicone OCA has been evaluated by several test protocols for use in electronic applications that require dynamic performance. In principle, silicone OCA is intrinsically more flexible than acrylic OCA due to the presence of two separate glass transition temperatures. It is capable of providing a variety of flexible features not currently offered by an acrylic OCA. The rheological properties were found to be key parameters to optimize elasticity, stress softening, creep, recovery, and bendability of silicone OCA, which should be in balance for easy removal of a fluorosilicone liner. Also, moisture and residual hydride could result in blistering in silicone OCA upon exposure to high temperature and high humidity but could be mitigated by proper modification of formulation and process conditions.

Acknowledgements

The authors would like to thank Kenta Suzuki, Tiberiu Siclovan and Roy Griswold for their insightful advices to design experiments and analyze the data as well as Mark Bisaillon and SongYi Ham for their help in preparing and testing the OCA samples.

References

1. Lee J.-H. et al. (2017) *Int J Adhesion Adhesives* pp.137
2. “OCA/OCR for Touch Panel – Market and Technology Analysis”, Displaybank, (2012) Nov
3. Benedek, I., Feldstein, M. ed. (2009) “Technology of Pressure-Sensitive Adhesives and Products”, CRC Press
4. Haq, J. et al. (2011) *Microelectronic Engineering* 88 pp.2852
5. Diani, J., Fayolle, B., Gilormini, P. (2009) *European Polym Journ*. pp.601
6. Sowa, D.; Czech, Z.; Byczynski, L. (2014) *Int. Journal Adh. Adj.* 49 pp.38-43
7. Moustafa, A. F. (2014) *Int J. Adhesion & Adhesives,* 50, pp. 65
8. Park C.; Kim H. (2015) *Polymer Science and Technology*, 26, pp. 313
9. Nakamura, K.; Mori, H. (2014) *Japan Adhesive Society*, 50, pp. 13
10. Walter Noll, “Chemistry and Technology of Silicones”, 2nd ed, Academic Press, Inc.